Crack Monitoring of Lock Infrastructure Using Strain Sensors

TRAVIS B. FILLMORE, BRIAN A. EICK and BILLIE F. SPENCER

ABSTRACT

Inland navigation systems facilitate barge traffic, the most efficient tonnage per fuel method of transportation. Miter gates allow barges to bypass navigational dams. The Dalles downstream miter gate has experienced numerous instances of cracking, threatening its continued operation and shipping on the Columbia River. The earliest instance of cracking led to the installation of a sensor system to ensure continued operation. The most recent serious cracking has resulted in serious efforts to track the cracking by moving some existing sensors and leveraging on-site underwater ROV cameras. A simple method is proposed to choose strain gage locations sensitive to cracks. A corresponding structural health monitoring algorithm to monitor the crack with strain gage data would benefit from supervised learning techniques. Thus, the existing strain gage system is leveraged to validate the finite element model, which in turn enables supervised learning techniques. It is found to be necessary to update the finite element model for acceptable validation.

INTRODUCTION

The United States (U.S.) navigation system connects many cities, with more than 25,000 miles of navigable inland waterways, much of which is maintained and operated by the United States Army Corps of Engineers (USACE). This allows barges to transport billions of dollars of goods annually. Barges are more efficient than trains and trucks [1]. Consequently, the U.S. inland navigation system forms an essential branch of infrastructure in the United States.

The U.S. inland navigation system includes a series of navigation locks and dams to enable barge traffic to move on each river. Many river sections, including the Columbia River do not naturally achieve depths necessary for barge traffic, necessitating dams. A series of navigational dams increase, stepwise, the depth of rivers, creating a set of pools deep enough for barge navigation. Locks help barges move past these dams and between pools. Lock failure or closure halts barge traffic, costing millions of dollars a day.

The Dalles miter gate is located on the Columbia River. It is a welded steel structure that is representative of miter gates maintained and operated by USACE. Figure 6 illustrates The Dalles miter gate boundary conditions under its two main load states, with major regions colored differently. The components of miter gates serve to facilitate locking events, and some of the main components are now defined. A miter gate is composed of two leaves. Each leaf of a miter gate has a top hinge called a gudgeon (colored blue in Figure 6) and a bottom ball-and-socket joint called a pintle (colored red in Figure 6). Each leaf swings open and is closed around the axis created by the gudgeon and pintle [2] [3] [4] [5].

Travis B. Fillmore, University of Illinois Urbana-Champaign, 205 N Mathews Ave, Urbana, IL 61801-2352, U.S.A.
Brian A. Eick Construction Engineering Research Laboratory, ERDC, 2902 Newmark Dr, Champaign, IL 61822-1078
Billie F. Spencer, University of Illinois Urbana-Champaign, 205 N Mathews Ave, Urbana, IL 61801-2352, U.S.A.

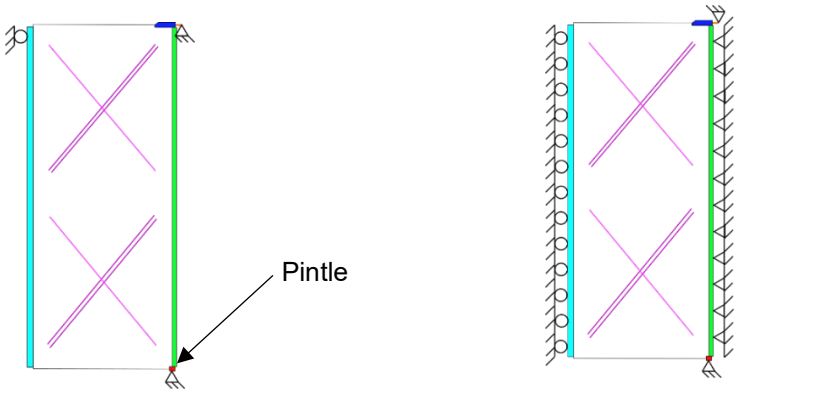

Figure 1. Load cases for The Dalles downstream miter gate. Blue represents the gudgeon, red represents the pintle, green represents the quoin, teal represents the miter, and magenta represents the diagonals.

When the lock chamber water height equals the downstream water height, hydrostatic pressure is absent, which is called the "Empty" load case. Figure 1(a) illustrates the boundary conditions for the Empty load case. The strut pushes the tops of the miter contact blocks together, the pintle resists the vertical gravity load, and the pintle and gudgeon resist horizontal load results from eccentricity of the gate center of mass from the axis of rotation.

When a miter gate acts as a damming surface it must hold water. Water applies hydrostatic pressure on the skin plate, with the greatest magnitude at the bottom. Hydrostatic pressure that pushes horizontally on the skin plate is analogous to loads on a floor system. In a floor system, loads travel from the slab to the girders and onward to the columns. The hydrostatic pressure in miter gate leaves is similar. For The Dalles miter gate, the hydrostatic pressure travels from the skin plate into the horizontal ribs/girders. Ideally, the load then travels through these horizontal girders and into the quoin contact block and finally the lock chamber wall.

The application of hydrostatic pressure causes the boundary conditions of the miter gate to change. When the lock chamber water height is higher than the downstream water height, hydrostatic pressure is present, which is called the "Full" load case. Figure 6(b) illustrates full load case boundary conditions. The hydrostatic pressure pushes the miter regions (colored teal in Figure 6) together so that they are restrained from moving perpendicularly to the lock wall. The hydrostatic pressure also pushes the quoin regions (colored green in Figure 6) into the lock wall so that friction prevents movement along the quoin once contact is made.

Several cracks were discovered on The Dalles miter gate South leaf in the pintle as shown in Figure 4. The cracks are large, with the skin plate crack measuring approximately 7 in. And the girder web crack measuring approximately 7.5 in. Since the pintle is an important boundary condition for the miter gate leaf, damage in it threatens to compromise gate function.

(a) Skin plate crack

(b) Girder web crack

Figure 2. Images of cracks in the pintle region of The Dalles miter gate South leaf. Photos courtesy of Garret Hall.

Decision-makers at The Dalles wanted to better track crack growth in their existing cracks. Options identified included crack gages [6] [7], soft elastomeric capacitors [8], acoustics emission testing [9], underwater ROV optical images, and reuse of existing strain gages. Section CRACK MONITORING OF THE DALLES MITER discusses crack monitoring procedures.

Due to the uniqueness of each miter gate, finite element (FE) models are necessary to utilize supervised machine learning algorithms. An FE model discretization needs to be verified to ensure numerical accuracy [10], which was previously performed for the FE model used in this study. Additionally, the FE model needs to be validated against the physical gate's behavior. An existing system of strain gages on the gate (with eight near the pintle) provided observations for validation. A subjective validation approach is adopted [11] where some uncertain boundary conditions are heuristically updated and a metric is defined that is judged qualitatively to indicate validity [12] [13]. This validation procedure is discussed in section VALIDATION AND MODEL UPDATING OF FINITE ELEMENT MODEL.

CRACK MONITORING OF THE DALLES MITER GATE

The time between the discussion of crack monitoring options and the lock outage to implement the crack monitoring options was only three months. Once on location, only three days would be given to install a crack monitoring solution. Therefore, a proven monitoring was desired since there was no time to prove a novel sensor. While the crack gage is proven in-the-dry, it would require waterproof sealing, meaning many layers of slow drying epoxy over the gage. Two technologies had already been proven on site: 1) a system of strain gages intended for structural health monitoring, and 2) an underwater ROV to take images of the bottom of the web crack. Therefore, it was decided to improve the ROV images using a painted grid onto the gate, with marks at every quarter inch. Therefore, the crack length and orientation could be much more reliably measured from the images.

Figure 3. Web crack with grid

While directly measuring the bottom of the web crack is helpful, it requires the crack to be clearly visible. This is not the case for the skin plate crack, which is permanently covered on both sides with retrofit plates. That leaves strain gages to monitor crack length on the skin plate crack. In order to optimize placement of the strain gages, some understanding of strain gage behavior is necessary. First, signal drift is common, necessitating some normalization to correct for drift. When the lock chamber fills and empties, the event is manifest in the strain gage readings with plateaus and flat valleys. The difference between adjacent plateaus and valleys is independent of drift, since the time scale is short. For a strain gage with a certain location and orientation, this can be represented by

$$E_{norm} = E_{full} - E_{empty}. \tag{1}$$

The sensitivity of the strain gage to crack growth can be represented by the metric of difference between this normalized strain between crack length j and crack length i:

$$S = E_{norm}^{(j)} - E_{norm}^{(i)}. \tag{2}$$

To clarify, several crack lengths are considered for the skin plate crack: $7, 10.5, 14.5, 18.5\ in.$, along the same orientation. So, if for a strain gage with a certain location and orientation measures strains at $7\ in.$ and $10.5\ in.$, sensitivity is given by $E_{norm}^{10.5\ in.} - E_{norm}^{7\ in.}$. The sensitivity must be greater than the strain gage noise threshold, which is approximately 10^{-6}.

Now, a single strain gage has been discussed, but we must consider many locations and orientations. In order to quickly and intuitively evaluate many locations for the skin plate strain gages to monitor crack growth, all reasonable locations are considered in parallel. The most reasonable location away from debris is inside the gate's interior retrofit, the so-called torsion box as illustrated in *Figure 4*.

Figure 4. Torsion box retrofit located inside the gate. The location crack through the plate behind the retrofit is indicated with a red line.

The plate in the same plane as the crack is the most reasonable place to put strain gages due to its proximity to the crack and relative shelter from underwater debris. To consider all locations on this plate, an FE simulation is run for the empty and load case for several skin plate crack lengths. The total simulation time is around 30 minutes. Strain fields are saved for postprocessing. Then, strain fields are processed as described in *(1)* and *(2)* for the whole plate. This is accomplished in Abaqus using the Visualization module toolbox named "Create New Field."

The resulting S for crack lengths $7\ in.$ and $10.5\ in.$ are shown in Figure 5. Notice that the scale is positive strain in the vertical direction. The minimum is 5×10^{-6} which is conservative relative to the noise threshold. This plot shows that a vertically oriented strain gage between the two middle bolts is sensitive to the $3.5\ in.$ of crack growth imposed. While the cases are not shown here, the same location and orientation is sensitive to crack growth from $10.5\ in.$ to $14.5\ in.$ and from $14.5\ in.$ to $18.5\ in.$

To reiterate, one FE simulation run is required as well as some postprocessing calculations and visual identification of high sensitivity areas. As a result of the simple and quick method, two strain gages were placed in the high sensitivity region oriented vertically within the short timeframe before the miter gate dewatering. Six additional strain gages were placed on the web of the girder near the girder crack. Two were placed in a sensitive region to web crack growth, while the others were located to demonstrate how the retrofit torsion box picks up load from the girder.

VALIDATION AND MODEL UPDATING OF FINITE ELEMENT MODEL

Decision-makers at The Dalles are interested not only in monitoring the status of the cracks, but also predicting future crack growth to plan future outages and repairs. Crack propagation can be predicted using FE models, however, a properly validated model is required to ensure that the miter gate behavior near the pintle is properly simulated.

In order to validate the FE model, a distribution of E_{norm} for each strain gage is found for a week of lock filling cycles resulting in a week of fillings/emptyings of the lock chamber. The output for the 32 strain gages from the FE model is

compared to the distributions. Then, the boundary conditions along the miter and quoin are modified to observe if the solution improved. The set of quoin and miter boundary conditions that produce strains that match the observation distributions best is taken as the updated and validated model.

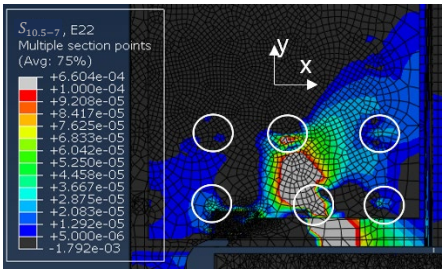

Figure 5. Sensitivity of strain gages to skin plate crack growth from 7 in. to 10.5 in. The hollow white circles are bolts.

While this validation was attempted before the sensors in the pintle region were moved, the strain gages located near the pintle were problematic. They were located near welds and exhibited unusual high magnitude readings. Therefore, validation and model updating was performed after the eight pintle strain gages were relocated. It was found that the FE strain gages near the bottom of the quoin and miter had somewhat higher or lower values than observed. If a gap exists, the strain gage near the gap will have a lower value and the strain gage at the end of the gap will have a larger value. A number of gaps were considered at the bottom of the quoin and miter. In order to evaluate which boundary condition situation gives the best result, we define an error metric. The set of simulated FE strains for the strain gages is taken as E_{norm}^{FE} and the set of the median of the observations for the strain gages is E_{norm}^{median}. The root mean squared relative error is

$$RMSRE\left(E_{norm}^{FE}, E_{norm}^{median}\right) = \sqrt{\frac{\sum\left(\frac{E_{norm}^{median} - E_{norm}^{FE}}{E_{norm}^{median}}\right)^2}{n}}, \tag{3}$$

Where n is the number of strain gages. The RMSRE for perfect quoin and miter boundary conditions is 0.943. The best result from heuristic model updating has a miter gap from the second rib from the bottom to the fifth, a quoin gap from the third girder from the bottom to the fifth, and another quoin gap from the twelfth girder from the bottom to the fourteenth. This improves the metric from the initial model with perfect contact's metric to 0.324. Likely further improvements to the RMSRE with automatic miter and quoin updating.

Correct behavior of the eight strain gages in the pintle near the cracks is of critical importance to training a successful machine learning algorithm to monitor the cracks. Unfortunately, one of the strain gages near the skin crack seems to be behaving somewhat erratically, with drifting visibly occurring during a single filling event. Therefore, that strain gage has been omitted from these results. The pintle strain gages are shown in Figure 6. Importantly, the RMSRE for strain gages near the pintle is 0.240 for the updated model whereas it is 0.413 for the pristine

model. Overall, the updated FE model is taken to be validated against those strain gages, producing reasonable values given the existing cracks.

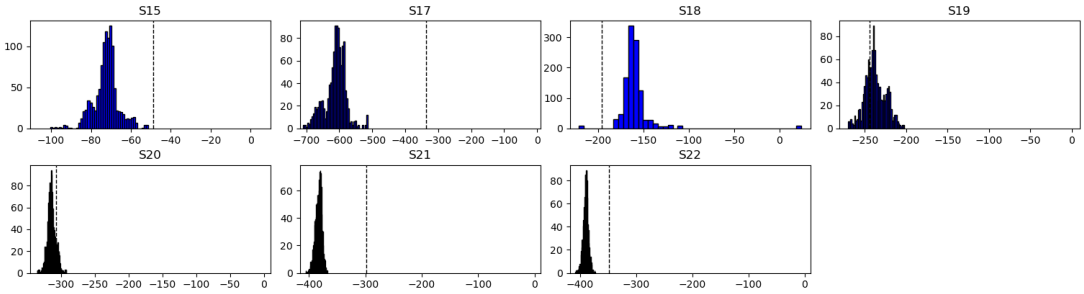

Figure 6. Eight pintle strain gages simulation results (vertical dashed line) versus distribution of observed results

CONCLUSION

Several large cracks were found at The Dalles miter gate. In order to monitor them, a simple method was utilized to find sensitive regions to crack growth, and shortly thereafter the channels were rerouted. Then an FE model was validated in preparation for development of crack monitoring algorithms. As part of this validation the FE model boundary conditions were updated, and the error was found to be small enough that the FE model is considered validated for crack monitoring purposes.

Therefore, it is ready to train a supervised machine learning algorithm to monitor the skin crack and the web crack. More advanced model updating algorithms may be employed to further improve the model performance relative to the strain gage observations.

ACKNOWLEDGEMENTS

The authors wish to thank Garrett Hall and Erica Tarbox for their knowledge and collaboration on The Dalles miter gate. Thanks are also due to Clayton Thurmer for assistance with moving the strain gages.

BIBLIOGRAPHY

[1] PricewaterhouseCoopers, "Economic contribution of the U.S. tugboat, towboat, and barge industry," Prepared for American Waterways Operators, Washington, D.C., 2017.

[2] USACE, "Design of hydraulic steel structures. Rep. No. 1110-2-2105.," USACE, Washington, D.C., 2014.

[3] PIANC, Miter gate design and operation, Brussels, Belgium: PIANC, 2017.

[4] R. Daniel and T. Paulus, Lock gates and other closures in hydraulic projects, Oxford, UK: Butterworth-Heinemann, 2019.

[5] R. A. Daniel, Miter gate design and operation, Saarbrucken, Germany: Lambert Academic Publishing, 2011.

[6] Omega, "Strain Gages to Measure Crack Propagation," 2023. [Online]. Available: https://sea.omega.com/tw/pptst/crack_propagation_strain_sg.html#description.

[7] HBM, "Crack Detection in Components," 2023. [Online]. Available: https://www.hbm.com/en/3453/rds-crack-propagation-gauges/?product_type_no=RDS:%20Crack%20Detection%20Gauges.

[8] S. A. Taher, J. Li, J.-H. Jeong, S. Laflamme, H. Jo, C. Bennett, W. N. Collins and A. R. Downey, "Structural Health Monitoring of Fatigue Cracks for Steel," *Sensors,* 2022.

[9] X. Yao, B. S. Vien, C. Davis and W. K. Chiu, "Acoustic Emission Source Characterisation during Fatigue Crack Growth in Al 2024-T3 Specimens," *Sensors,* 2022.

[10] T. B. Fillmore and M. D. Smith, "Behavior of Flexible Pintles for Miter Gates," *Journal of Waterway, Port, Coastal, and Ocean Engineering,* vol. 147, no. 5, 2021.

[11] R. G. Sargent, "Verification and validation of simulation models," in *Proceedings of the 2011 Winter Simulation Conference*, 2011.

[12] S. Wang, C. Rodgers, T. B. Fillmore, B. Welsh, T. S. S. A. V. Golecki, B. A. Eick and B. F. Spencer, "Vision-based model updating and evaluation of miter gates on inland waterways," *Engineering Structures,* vol. 280, 2023.

[13] T. Marwala, Finite-element-model updating using computional intelligence techniques: Applications to structural dynamics, London: Springer , 2010.